Proceedings of the ASME 2010 3rd Joint US-European Fluids Engineering Summer Meeting and 8th International Conference on Nanochannels, Microchannels, and Minichannels
FEDSM-ICNMM2010
August 1-5, 2010, Montreal, Canada

FEDSM-ICNMM2010-30220

BED HEIGHT EFFECTS ON FLUIDIZED BED HYDRODYNAMICS

David R. Escudero and Theodore J. Heindel*
Department of Mechanical Engineering
Iowa State University
Ames, Iowa 50011

ABSTRACT

Characterizing the hydrodynamics of a fluidized bed is of vital importance to understand the behavior of these multiphase flow systems. Minimum fluidization velocity and gas holdup are two important factors used to understand the hydrodynamics of a fluidized bed. Experimental studies on the effects of bed height on the minimum fluidization velocity and gas holdup were carried out using a 10.2 cm diameter cylindrical fluidized bed filled with 500-600 μm glass beads. In this study, four different bed height-to-diameter ratios were used: H/D = 0.5, 1, 1.5, and 2. Minimum fluidization velocity was determined for each H/D ratio using pressure drop measurements. Local time-average gas holdup was determined using non-invasive X-ray computed tomography imaging. Results show that minimum fluidization velocity is not affected by the change in bed height, while local gas holdup does appear to be affected by the change in bed height.

Keywords: bed height, fluidized bed, gas holdup, minimum fluidization velocity, X-ray computed tomography.

INTRODUCTION

Fluidized bed hydrodynamic behavior is very complex and must be understood to improve fluidized bed operations. One of the most important parameters to characterize fluidized bed conditions is the minimum fluidization velocity (U_{mf}) [1], which is related to the drag force needed to attain solid suspension in the gas phase. The minimum fluidization velocity also constitutes a reference for evaluating fluidization intensity when the bed is operated at higher gas velocities [2]. In general, U_{mf} is a function of particle properties/geometry, fluid properties, and bed geometry.

Sau et al [3] determined the minimum fluidization velocity for a gas-solid system in a tapered fluidized bed and studied the effects that bed geometry, specifically the tapered angle, had on the minimum fluidization velocity. They used three different angles (4.61º, 7.47º, and 9.52º) to observe the effect on minimum fluidization velocity. Results showed that as the tapered angle increased, U_{mf} increased, which implied a dependence of the minimum fluidization velocity to the geometry of the fluidized bed. Moreover, Hilal et al. [4] analyzed the effects of bed diameter, gas distributor, and inserts on minimum fluidization velocity. It was shown that both the bed diameter and the type and geometry of the distributor affected U_{mf}. For example, U_{mf} increased with an increase in the number of holes in the distributor plate. Furthermore, with an increase in the bed diameter there was a decrease in U_{mf}. Finally, the insertion of tubes along the fluidized bed reduced the effective cross-sectional area for fluidization, which produced a high interstitial gas velocity causing a decrease in U_{mf}.

The influence of bed height on minimum fluidization velocity has been studied using different types of fluidized beds. Zhong et al. [5] completed minimum fluidization experiments in spouted fluidized beds. In a spouted fluidized bed, the bed chamber is tapered like a funnel, which creates different hydrodynamics, and the fluidization air is typically injected through a single orifice. Zhong et al. [5] used a two dimensional spouted fluidized bed with dimensions 300 mm × 30 mm and a height of 2000 mm, and fluidized a variety of Geldart Type-D particles (mung beans, polystyrene, millet). Filling the bed with these materials to different heights (300-550 mm), they determined the minimum spouting fluidization velocity, defined as the minimum superficial gas velocity at

* Corresponding Author: T.J. Heindel, theindel@iastate.edu

which the spout initiates in the central region and the surrounding annulus is fluidized; this is analogous to minimum fluidization velocity in a bubbling fluidized bed. They concluded that the static bed height for a spouted bed influenced the minimum spouting fluidization velocity; increasing the bed height increased the spouting velocity.

Sau et al. [2] used a gas-solid conical tapered fluidized bed to find the minimum fluidization velocity and the pressure drop across the bed. The dimensions of the fluidized bed at the bottom were 48, 42, and 50 mm, the top of the bed measured 132, 174, and 212 mm, and the column heights were 520, 504 and 483 mm, respectively. They concluded that bed height for this type of bed did not have a significant effect on the minimum fluidization velocity, i.e., U_{mf} was independent of bed height for this type of conical tapered fluidized bed.

Ramos et al. [1] studied the minimum fluidization velocity for gas-solid 2D fluidized beds. They used a rectangular bed (1 × 0.2 × 0.012 m) filled with glass beads of three different diameters (160-250, 250-400, and 490-700 μm) and various bed heights (2, 4, 8, 16, 20, 40, and 60 cm). Their results revealed that as the static bed height increased, U_{mf} increased.

Gunn and Hilal [6] studied gas-solid fluidized beds using glass beads with beds that had 89 and 290 mm ID. The glass beads diameters were 100 and 500 μm. They used four different bed heights (20, 30, 40, 50 cm). The results for minimum fluidization velocity showed that for all the material and experimental conditions used in this study there was no significant change in the minimum fluidization velocity when the bed height was increased. Therefore, U_{mf} was independent of bed height.

Cranfield and Geldart [7] studied the fluidization characteristics of large particles (1000-2000 μm) of alkalized alumina in a fluidized bed with a cross-sectional area of 61×61 cm at different bed heights (5, 10, 15, 20, 25, and 30 cm). They showed that for 3D beds, the minimum fluidization velocity remained constant no matter the bed height used in the experiments.

Gas holdup is another important parameter that characterizes fluidization quality, homogenous mixing, and process efficiency in a fluidization system, and is defined as the volume fraction of gas present within the bed. Using an optical probe, Zhu et al. [8] determined the solid concentration (the inverse of gas holdup) in a gas-solid system for bubbling and turbulent fluidization regimes. Results showed that the turbulent regime solid concentrations are not uniform in the axial and radial direction, showing a nonuniformity of the flow structure. In the bubbling regime, the nonuniformity increases as the superficial gas velocity also increases.

Moreover, Zhu et al. [8] studied the effects that changing the static bed height had on the solid concentration. Results showed that increasing the static bed height produced an increase in the solid concentrations mainly in the central region of the bed, while the wall region had no significant changes. This phenomenon is attributed to the increased presence of bubbles in the material as the bed height increased.

Du et al. [9] measured the solid concentration for a turbulent fluidized bed. Results showed that at high gas velocities, especially in the turbulent regime, the cross-sectional solids holdup exhibits a radial symmetric distribution, while this is not the case for the bubbling regime. At low gas velocities in the bubbling regime, dispersed bubbles yield a lower solids concentration in the center of the bed. The asymmetric distribution of solids concentration was attrributed to the spiral motion of bubbles in the bed.

X-ray computed tomography (CT) generates a 2D image of the object of interest. X-rays passed through the object and the intensity values are recorded at several projections by an imaging device. After the images are collected, computer algorithms reconstruct the images to produce a 3D projection of the object. However, due to the number of projections that must be acquired in order to obtain a whole reconstruction of the object, this technique does not have good temporal resolution. Conversely, having multiple scans from different projections give a high spatial resolution to this technique, a characteristic that can be used to measure the time-average local gas holdup anywhere within the imaging volume in a very efficient way.

X-ray CT is widely used in measuring multiphase flow characteristics. Franka et al. [10] used X-ray CT in four different materials (glass beads, melamine, ground walnut shell, and ground corncob) to visualize and compare the fluidization structure between the materials. Results showed that in terms of fluidization uniformity, glass beads fluidize symmetrically about the center of the bed and maintain a constant uniformity as the gas velocity increased while less dense melamine, ground walnut shell, and ground corncob show regions where jetting, spouting, and channeling effects appeared and decreased the bed uniformity. However, as gas velocity increased the uniformity of the non glass materials increased too, obtaining a better gas distribution inside the material.

Moreover, X-ray CT images and data allow the calculation of time-average local gas holdup or solid holdup. Grassler and Wirth [11] used X-ray CT to determine the solids concentration in a 0.19 m diameter circulating fluidized bed with 50-70 μm glass beads as the bed material. Tests were carried out in two different systems. In the first, solid concentrations were calculated with an up flow system. Results for this system showed that radial solid concentration exhibited a parabolic shape with a maximum concentration close to the wall of the reactor and a minimum concentration in the center of the bed. For the second, the solid concentration was calculated with a down flow system. For this case, the solid concentration distribution was much more complex and depended upon the gas-solid distributor operating conditions. Results showed various solid concentration distributions from a homogeneous distribution with a parabolic profile to concentrated strands in the center of the bed. Finally, the study also showed that the solids concentration was accurately calculated within 5% error for concentrations up to 20 vol% with a minimum spatial resolution of 0.2 mm.

Franka and Heindel [12] studied the effects of side air injection, superficial gas velocity, and bed material had on the local time-average gas holdup in a 10.2 cm fluidized bed, using X-ray computed tomography. Using different materials (glass beads, ground corncob, and ground walnut shell), superficial gas velocities (U_g), and side air injection flow rates (Q_{side}), they determined the variations on the fluidization hydrodynamics of the bed. They found that with side air injection, the side air flow rose near the wall but then expanded into the bed as height and Q_{side} increased. As U_g increased, the effects caused by the side air injection were less pronounced, and the overall gas holdup in the system increased. Fluidization among the different materials had similar behaviors with some notable differences. Side air injection was less influential on the less dense material and gas holdup was lowest for the denser material. Finally, they demonstrated the usefulness of X-ray computed tomography in visualizing the internal features of fluidized beds.

The goal of this paper is to determined the effects caused by varying the bed height on the hydrodynamics behavior in a 3D cylindrical fluidized bed.

EXPERIMENTAL SETUP

The reactor used in these experiments is a cold flow fluidized bed reactor. The cylindrical fluidized bed was fabricated with 10.2 cm internal diameter (ID) acrylic with a 0.64 cm wall thickness. As shown in Figure 1, the reactor consists of three main chambers: the top chamber or freeboard region, the bed chamber, and the plenum. Fluidization occurs in the bed chamber which is 30.5 cm tall and 10.2 cm ID. Square flanges (16.5×16.5 cm) connect each section. An aeration plate is located immediately below the bed chamber; it is fabricated from a 1.27 cm thick acrylic plate with 62, 1 mm diameter holes spaced approximately 1.27 cm apart in a circular grid for a total open area of 0.62%. To avoid material blocking the aeration holes, a 45 mesh screen with openings of 0.04 cm is attached to the plate using silicone adhesive.

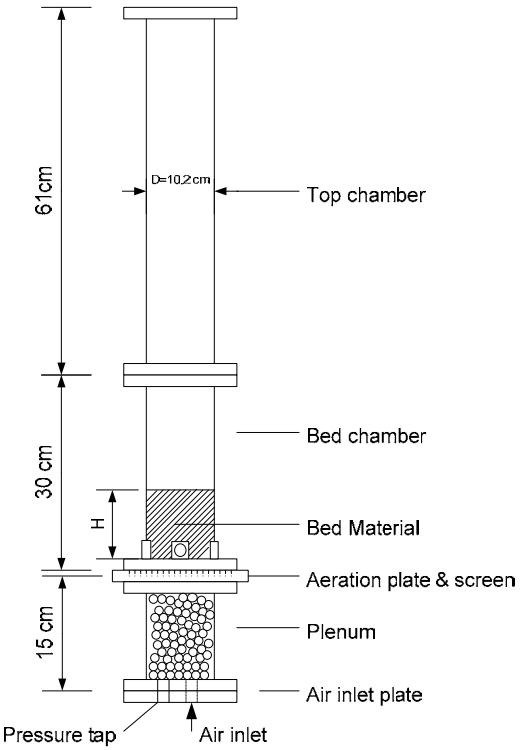

FIGURE 1: FLUIDIZED BED REACTOR (NOT TO SCALE). THE STATIC BED HEIGHT IS IDENTIFIED BY H.

Compressed air from the laboratory's building air supply is used as the fluidizing gas for this research. The pressure at which the compressed air is delivered inside the laboratory is 620 kPa (90 psi). However, since the flow rates used for fluidization vary depending of the specific conditions of each experiment, an air flow control board with four independent air lines is used to deliver the required air to the fluidized bed.

The fluidized bed air flow is regulated by a manual stainless steel pressure regulator and attached filter, with a pressure range of 0-862 kPa (0-125 psi) and maximum inlet pressure of 2.07 MPa (300 psi). The regulated air flows through one of two mass flow meters: a 0-1000 Lpm stainless steel Aalborg GFM771 flow meter, which is used for high gas flow applications, and a 0-200 Lpm Aalborg GFM571 flow meter, used in lower gas flow applications. This allows for better measurement resolution. The flow through the respective mass flow meter is controlled through ball valves.

Pressure is measured with a Dwyer 0-34.5 kPa (0-5 psig), 4-20 mA output pressure transducer located in the bottom of the plenum. The signals obtained from the pressure transducer and mass flow meters are connected to a computer controlled data acquisition system. Average measurements were necessary due to the highly variable pressure signal caused by the bubbling fluidized bed. In this study, data collection occurred at a rate of 1000 Hz for a time interval of 5 seconds, average pressure, and average flow rate were subsequently written to a data file.

The fluidizing material used in this study was 500-600 µm glass beads (ρ_{glass} = 2600 kg/m^3). The bed bulk density was determined knowing the material mass and the static bed volume. Bed material was slowly added until the desired static bed height was determined, which corresponded to H/D = 0.5, 1, 1.5, and 2. Before the bed height was measured, the bed was fluidized and then allowed to collapse to avoid any packing effects due to the filling process. The material mass was then measured and the given bed bulk density was calculated. Table 1 summarizes the characteristics of the various glass bead systems used in this study.

TABLE 1: BED MATERIAL PROPERTIES.

	Glass Beads	
H/D	**Bed Mass (g)**	**Bulk density (kg/m^3)**
0.5	590	1411±30
1	1180	1412±30
1.5	1775	1419±30
2	2440	1464±30
Diameter (µm)	500-600	
Particle Density (kg/m^3)	2600	

To avoid electrostatic effects that may build up during fluidization, the fluidization air is passed through a humidifier before entering the fluidized bed inlet. Several trials in the laboratory have shown that using this simple solution completely eliminated electrostatic effects.

The minimum fluidization velocity is defined as the minimum superficial gas velocity where particle fluidization is achieved. Minimum fluidization velocity is determined using the following pressure measurement procedure. First, the reactor is filled with the desired material to a specified height. Air at U_g= 40.8 cm/s is passed through the bed for about an hour to condition the system; this process is repeated each time the material is replaced. After the conditioning period, the pressure and flow rate are acquired using the DAQ system. Data are collected at 1000 Hz over a 5 second interval, averaged over this period, and then output to an Excel file. Next, the air flow rate is decreased by 1 cm/s by closing the pressure regulator. After waiting 60 seconds, a period such that the bed is in a quasi steady state, the pressure and flow rate are again averaged over a 5 second interval. This process is repeated until the flow rate reaches U_g= 0 cm/s; at this point the test is completed. For statistical purposes, each test for the specified bed height is repeated 5 times.

After all the bed material data are collected, the same procedure is repeated in an empty reactor. This is done to quantify the pressure drop through the aeration plate and plenum. The empty reactor pressure data are then subtracted from the fluidized bed data at the respective superficial gas velocity. Since the flow rates between the empty reactor and fluidized bed tests do not match exactly, a linear interpolation method is employed to calculate the empty bed pressures corresponding to the fluidized bed flow rates. Finally, the bed pressure drop is plotted as a function of superficial gas velocity and the minimum fluidization velocity is defined as the point in which the pressure drop across the bed remains constant. Figure 2 shows a sample plot obtained for glass beads where the static bed height corresponds to H/D =1.

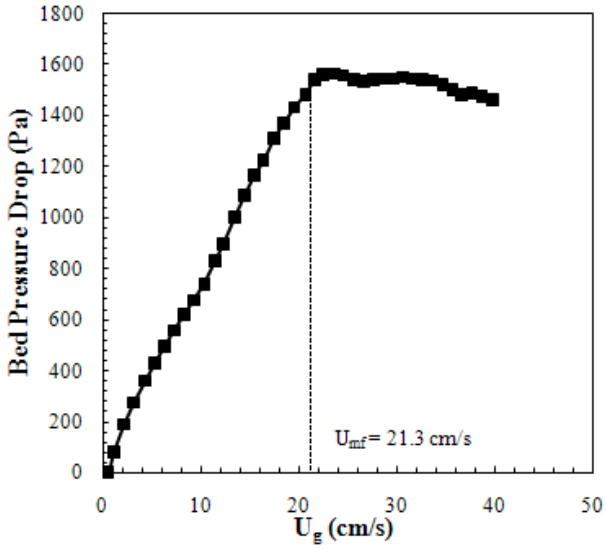

FIGURE 2: SAMPLE MINIMUM FLUIDIZATION PLOT FOR GLASS BEADS WITH H/D = 1.

X-ray computed tomography (CT) scans are captured for the different H/D ratios (0.5, 1, 1.5, 2) and different superficial gas velocities U_g =1.25, 1.5, 1.75, 2, 3 U_{mf}. CT imaging allows for the quantitative analysis of the local time-average gas holdup to determine the effects of different bed heights on the hydrodynamic behavior of the fluidized bed.

The X-ray facility used in this study has been described elsewhere [12-14], and only the procedure used in this study is described here. First, the X-ray source that is located opposite to the CT detector is warmed up at the same time the thermoelectric cooler on the camera is simultaneously cooled to 0°C to reduce noise and allow for long CT scans. After the warm-up process is finished, the X-ray power, such as voltage and current, exposure time, and binning are adjusted based on the bed material in the imaging region. For this study, the power remained constant for all conditions with a voltage of 150 keV and a current of 3.5 mA, while the exposure time is set to 1 second and the binning is set to 4×4.

Next, the fluidized bed is placed in the imaging region and the scintillation crystals in the detector are excited with X-rays for approximately 20 minutes. The fluidized bed is positioned in the same horizontal location for all bed heights. However, as the H/D ratio increased, it is necessary to move the bed stand down so that all the bed material can be located within the imaging region. CT scan settings are adjusted; including the number of vertical slices (horizontal cross-sections), slice

interval, and slice start location. Once the settings are adjusted, the system is ready to start a CT scan.

The gas holdup (void fraction or volumetric gas fraction) describes the amount of voidage in the bulk material. Quantifying the local time-average gas holdup, ε_g, requires the CT intensity of the empty reactor (I_g), a CT intensity of the reactor filled with a fixed bed of the bulk material (I_b), and a CT intensity of the reactor under specified fluidization conditions (I_f). To ensure the same response for each condition from the detector system, each CT is taken with the same X-ray source power settings for the respective conditions.

The local time-average gas holdup is then determined from the two reference CT images and the flow CT image [12]:

$$\varepsilon_g = \frac{I_f - I_b + \left(I_g - I_f\right)\left(\varepsilon_{g,b}\right)}{I_g - I_b} \quad (1)$$

where the bulk void fraction, $\varepsilon_{g,b}$, is defined as:

$$\varepsilon_{g,b} = 1 - \frac{\rho_b}{\rho_p} \quad (2)$$

where ρ_b and ρ_p are the bulk and particle density, respectively. The bulk density is determined experimentally and the particle densities are given by the manufacturer. This calculation results in a 3D image mapping the time-average gas holdup in the reactor.

RESULTS AND DISCUSSION

Minimum Fluidization Velocity

Figure 3 shows the bed pressure drop as a function of superficial gas velocity for 500-600 μm glass beads at different H/D ratios. Bed pressure drop increases when the H/D ratio is increased because, for the constant diameter fluidized bed, increasing the bed height increases the bed mass.

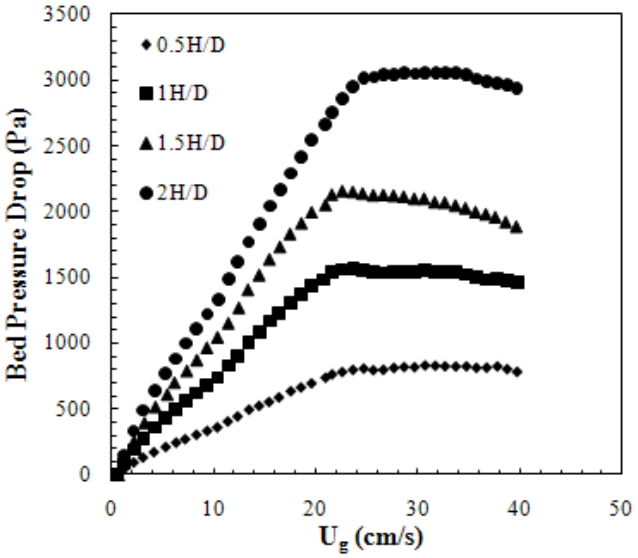

FIGURE 3: BED PRESSURE DROP AS A FUNCTION OF SUPERFICIAL GAS VELOCITY.

Minimum fluidization velocity, on the other hand, did not show significant changes when the H/D ratio increased. This is apparent when a force balance between the gravity and pressure force is used to identify the minimum fluidization velocity, which is identified as the velocity when these two forces are equal. As shown in Figure 4, the knee of the graphs (U_{mf}) is approximately constant for all bed heights considered here. However, the values of the bed pressure force over the bed weight that surround the knee of the graph are not identically 1 due to wall friction forces presented in the fluidized bed. Furthermore, at higher superficial gas velocities, the ratio between bed pressure force and bed weight shows a slight decrease, which is attributed to the effects of friction forces on the fluidized bed wall.

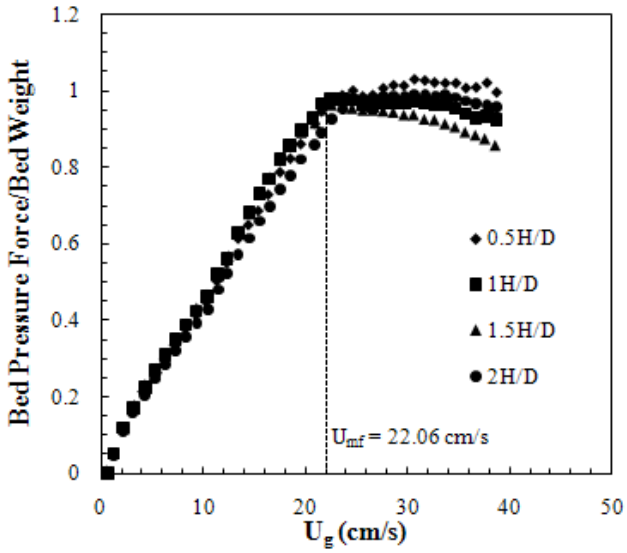

FIGURE 4: BED PRESSURE FORCE/BED WEIGHT AS A FUNCTION OF SUPERFICIAL GAS VELOCITY.

Local time-average gas holdup

The 3D time-average gas holdup obtained from Eq. (1) can be viewed anywhere within the fluidized bed [12]. Images of y-slice and z-slice gas holdup at specific superficial gas velocities for different H/D ratios are presented in Figures 5 and 6; y-slice images are taken in the center of the bed, while z-slice images are taken at two different axial heights (h = 2.5 cm and 5.1 cm) to show how fluidization structure and gas holdup change with increasing superficial gas velocity and increasing H/D ratio. When $U_g = 1.25U_{mf}$ (Figure 5), the gas holdup map is similar for all H/D values. Observing the three different slices at H/D= 0.5, the range of the values of gas holdup are between 0.4 and 0.5, the highest local gas holdup is located around the walls of the reactor. As H/D increases, the flow structure is similar. Differences in the surface profile are observed when $U_g = 3U_{mf}$ (Figure 6).

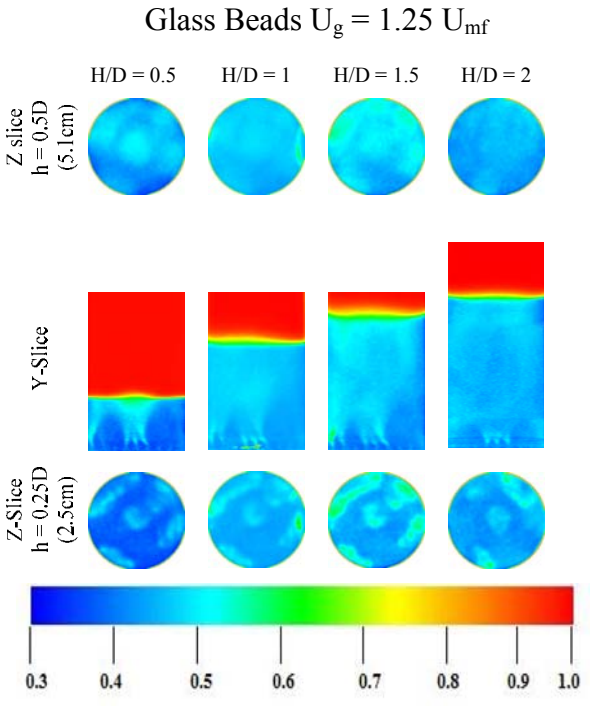

FIGURE 5: GAS HOLDUP Y- AND Z-SLICES FOR U_g = 1.25U_{mf} AT DIFFERENT H/D RATIOS.

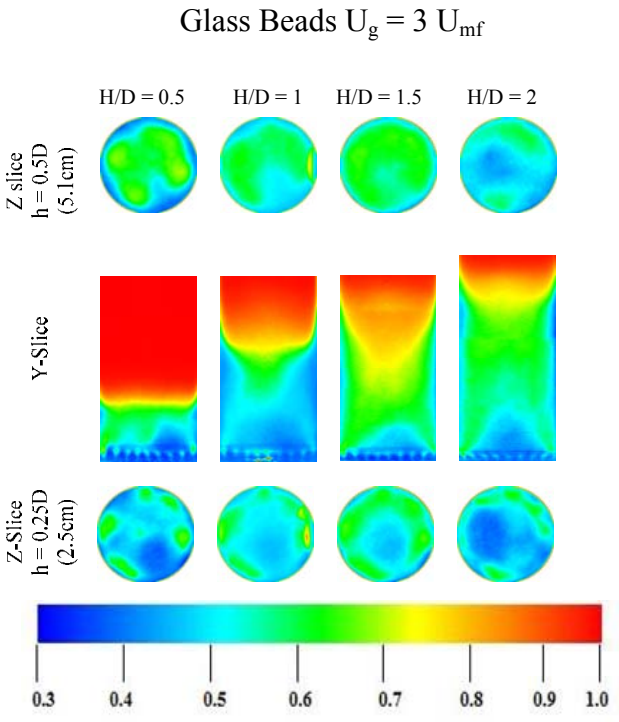

FIGURE 6: GAS HOLDUP Y- AND Z-SLICES FOR U_g = 3U_{mf} AT DIFFERENT H/D RATIOS.

Jetting from individual aeration holes is observed in the y-slice images in Figures 5 and 6. It is observed that increasing U_g increases the number of active aeration holes. Additionally, increasing U_g decreases the jet length because mixing in the fluidized bed increases and the individual jets lose their identify.

Regions of low gas holdup are shown in Figure 6 near the bottom center of the bed. As the bubbles rise, they coalesce and migrate towards the bed center, increasing the gas holdup in this region. The large bubbles erupt from the bed near the center, throwing glass beads against the wall, which fall back into the bed. These hydrodynamics create high gas holdup regions near the top center of the bed while lower gas holdup regions (higher solids concentration) are found along the bed walls. Increasing the H/D ratio allows for additional bubble coalesce creating slugs inside the bed, which rise in the bed center, enhancing the gas holdup differences near the top of the bed.

The y- and z-slices images shown in Figures 5 and 6 reveal qualitative information about the bed hydrodynamics. The actual gas holdup values within the bed are used to obtain quantitative information. Figure 7 shows the local time-average gas holdup plotted as a function of location along two mutually perpendicular lines that pass through the bed center for the four H/D ratios tested with U_g = 1.25U_{mf} and at an axial height of h = 0.25D (2.5 cm). Figure 7A shows the local gas holdup data along the y-slice, while Figure 7B shows the data along the x-slice. The local rise and fall in gas holdup is attributed to the presence of jets from the aeration plate. Overall, the trends for the different H/D ratios are similar.

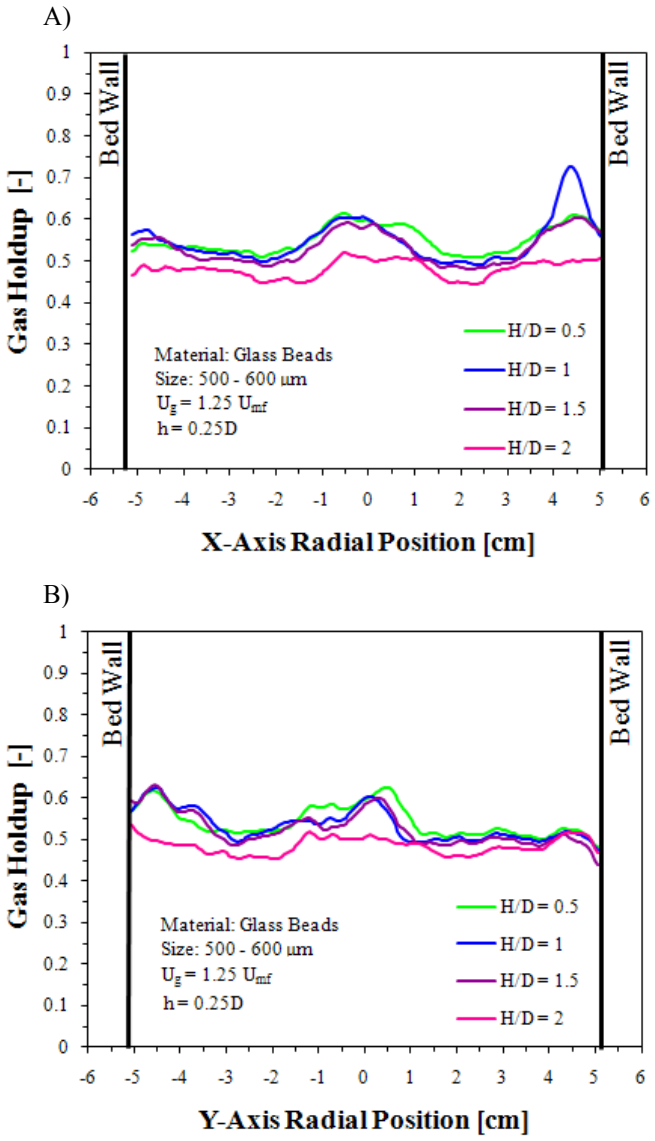

FIGURE 7: LOCAL GAS HOLDUP AS A FUNCTION OF SPATIAL LOCATION AT h = 0.25D: A) Y-SLICE AND B) X-SLICE.

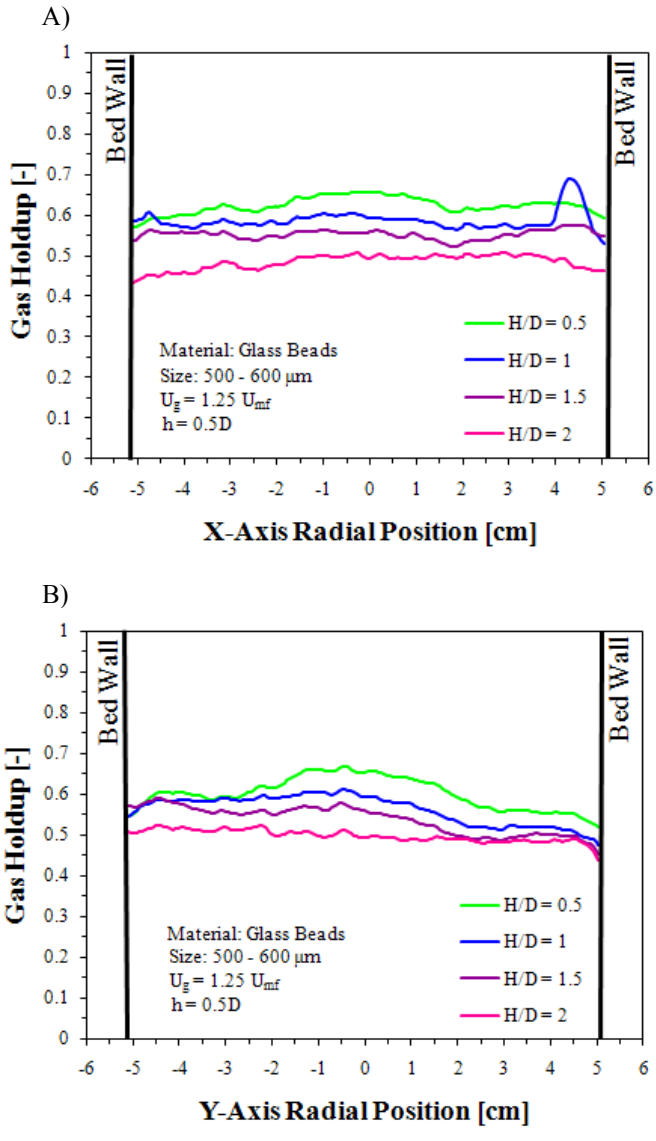

FIGURE 8: LOCAL GAS HOLDUP AS A FUNCTION OF SPATIAL LOCATION AT h = 0.5D: A) Y-SLICE, AND B) X-SLICE.

Figure 8 shows the local time-average gas holdup for $U_g = 1.25U_{mf}$ at h = 0.5D (5.1 cm) along the same two planes. Increasing the height from the aeration plate diminishes the variations in local gas holdup. There is a slight decrease in gas holdup as the H/D ratio increases due to the increase in bed mass above this location hindering bed expansion. For example, at H/D = 0.5, the bed can freely expand at h = 0.5D, whereas with H/D = 1, expansion is suppressed.

The local gas holdup values can be averaged across a horizontal slice to show how gas holdup varies with bed height. Figure 9 shows the horizontal spatial-average and time-average gas holdup for H/D = 1.5 as a function of different superficial gas velocities. There is an increase in the overall gas holdup with an increase in superficial gas velocity. This effect is attributed to the higher volume of air that is passing through the bed material. This trend is observed for all the H/D ratios tested in this study.

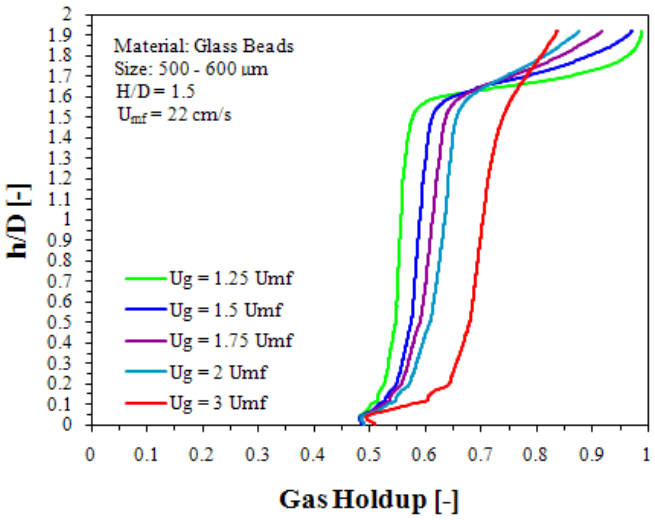

FIGURE 9: EFFECT OF SUPERFICIAL GAS VELOCITY ON SPATIALLY-AVERAGED AND TIME-AVERAGE GAS HOLDUP FOR DIFFERENT U_g VALUES AT H/D = 1.5.

CONCLUSIONS

Minimum fluidization velocity was determined over a range of bed heights using a 10.2 cm diameter fluidized bed filled with 500-600 µm glass beads. For the conditions of this study, the minimum fluidization velocity was independent of bed height; the results obtained in this research using a 3D fluidized bed corroborate the data presented in the literature.

Local time-average gas holdup information was calculated using X-ray computed tomography images at different flow and bed height conditions. As superficial gas velocity increased, the overall gas holdup increased for every H/D ratio studied. Flow behavior was also affected with the increase in superficial gas velocity. Increasing the H/D ratio, particularly at the higher gas flow rates, enhanced bubble coalescence creating slugs that flow thorough the center of the bed, producing regions of low gas holdup near the walls of the fluidized bed.

Future studies will address the effects of material density on gas holdup for the same flow and bed height conditions.

ACKNOWLEDGMENTS

This work was supported through a Fulbright Scholarship and Iowa State University. The X-ray facility used in this research was funded by the National Science Foundation under award number CTS-0216367 and Iowa State University.

REFERENCES

[1] Ramos Caicedo, G., García Ruiz, M., Prieto Marqués, J. J. and Guardiola Soler, J. (2002). "Minimum fluidization velocities for gas-solid 2D beds." *Chemical Engineering and Processing,* **41**(9): 761-764.

[2] Zhong, W., Jin, B., Zhang, Y., Wang, X. and Xiao, R. (2008). "Fluidization of biomass particles in a gas−solid fluidized bed." *Energy & Fuels,* **22**(6): 4170-4176.

[3] Sau, D. C., Mohanty, S. and Biswal, K. C. (2007). "Minimum fluidization velocities and maximum bed pressure drops for gas-solid tapered fluidized beds." *Chemical Engineering Journal,* **132**(1-3): 151-157.

[4] Hilal, N., Ghannam, M. T. and Anabtawi, M. Z. (2001). "Effect of bed diameter, distributor and inserts on minimum fluidization velocity." *Chemical Engineering and Technology,* **24**(2): 161-165.

[5] Zhong, W., Chen, X. and Zhang, M. (2006). "Hydrodynamic characteristics of spout-fluid bed: Pressure drop and minimum spouting/spout-fluidizing velocity." *Chemical Engineering Journal,* **118**(1-2): 37-46.

[6] Gunn, D. J. and Hilal, N. (1997). "The expansion of gas-fluidised beds in bubbling fluidisation." *Chemical Engineering Science,* **52**(16): 2811-2822.

[7] Cranfield, R. R. and Geldart, D. (1974). "Large particle fluidisation." *Chemical Engineering Science,* **29**(4): 935-947.

[8] Zhu, H., Zhu, J., Li, G. and Li, F. (2008). "Detailed measurements of flow structure inside a dense gas-solids fluidized bed." *Powder Technology,* **180**(3): 339-349.

[9] Du, B., Warsito, W. and Fan, L.-S. (2003). "Bed nonhomogeneity in turbulent gas-solid fluidization." *AIChE Journal,* **49**(5): 1109-1126.

[10] Franka, N. P., Heindel, T. J. and Battaglia, F. (2007). Visualizing cold-flow fluidized beds with x-rays. *ASME International Mechanical Engineering Congress and Exposition*. Seattle, Washington, ASME**:** 7.

[11] Grassler, T. and Wirth, K. E. (2000). "X-ray computer tomography - potential and limitation for the measurement of local solids distribution in circulating fluidized beds." *Chemical Engineering Journal,* **77**(1): 65-72.

[12] Franka, N. P. and Heindel, T. J. (2009). "Local time-averaged gas holdup in a fluidized bed with side air injection using X-ray computed tomography." *Powder Technology,* **193**(1): 69-78.

[13] Franka, N. P. (2008). "Visualizing fluidized beds with X-rays". MS Thesis, Department of Mechanical Engineering, Iowa State University, Ames, IA.

[14] Heindel, T. J., Gray, J. N., and Jensen, T. C. (2008). "An X-Ray System for Visualizing Fluid Flows," *Flow Measurement and Instrumentation*, **19**(2): 67-78